Using Geodetic GPS Receivers to Measure Vegetation Water Content

Wei Wan (1)
Kristine M. Larson (2)
Eric E. Small (3)
Clara C. Chew (3)

1. School of Earth and Space Sciences, Peking University, Beijing, China
2. Department of Aerospace Engineering Sciences, University of Colorado, Boulder
3. Department of Geological Sciences, University of Colorado, Boulder

Abstract

A GPS-based method is presented to measure vegetation water content. Commercially available geodetic-quality GPS receivers and antennas are used. The method is tested using GPS measurements collected over three field seasons. The GPS data are compared with *in situ* data for three plant types: desert grass, wheat and alfalfa. The GPS retrievals or vegetation water content are based on the GPS signal-to-noise ratio (SNR) data. Instrumental issues that affect the SNR data are discussed, particularly satellite transmit power variations, footprint variations, and temperature effects. The amplitudes of the SNR data show a nearly linear relationship to the water content in grasses (0-0.5 kg/m^2) and wheat crops (0-0.9 kg/m^2). As predicted by theory, this simple linear relationship breaks down in vegetation with heavy water content, such as alfalfa. The field results are consistent with forward model predictions, which effect restricts the use of this simple linear model for vegetation to water content of less than ~1 kg/m^2.

Introduction

The primary use of the GPS constellation is real-time navigation; a much smaller community uses the same signals with advanced instruments and analysis tools for precise positioning applications such as geoscience fields such as geodesy, geophysics, and glacier dynamics, see e.g. Segall and Davis (1997). Since it was first suggested by Martin-Neira (1993), reflected GPS signals are also being used by geoscientists. Many of the early GPS reflection experiments were focused on altimetry (Garrison and Katzberg 2000; Gleason et al. 2005), ocean winds (Garrison et al. 2002) and soil moisture (Katzberg et al. 2005). More recently, vegetation growth has been the focus of GPS reflection studies (Egido et al. 2012; Rodriguez-Alvarez et al. 2011; Rodriguez-Alvarez et al. 2012). While the details associated with how these instruments were deployed and how the data were analyzed varies, all were designed to measure reflections. An alternative GPS reflection method, GPS-IR (GPS Interferometry Reflectometry), uses reflections that are measured by geodetic-quality GPS instruments. These instruments were not designed to measure reflections. However, it has been shown that they provide consistent measurements of upper surface soil moisture content, snow depth, and coastal sea level (Larson et al. 2008; Larson et al. 2009; Larson et al. 2013).

Small et al. (2010) first showed a qualitative agreement between reflections recorded by geodetic-quality GPS receivers and vegetation growth; however, they did not attempt a quantitative analysis. Chew et al. (in revision) recently developed an electrodynamic model that simulates GPS reflections in the presence of varying soil moisture and vegetation cover. This study showed that a nearly linear relationship should exist between GPS measurements and vegetation water content up to ~1 kg/m^2. Beyond this value, the relationship becomes non-linear and can no longer be used to predict changes in vegetation in a forward sense. Additionally, it was shown that soil moisture's effect on GPS measurements should introduce a 0.1-0.2 kg/m^2 error in vegetation water content estimation.

Chew et al. (in revision) validated their theoretical results with *in situ* data, but did not consider systematic errors in the GPS retrievals, nor did they consider the practical limitations associated with using a geodetic GPS system to measure vegetation water content. The goal of this paper is

to explore the technical issues that must be resolved in order to use GPS-IR to measure vegetation water content. *In situ* measurements of both grasslands and agricultural crops are used to validate the GPS retrievals of vegetation water content.

GPS Interferometry Reflectometry

In the GPS-IR technique the Signal to Noise Ratio (SNR) data are used to infer environmental characteristics (Larson et al 2008; Larson et al; 2009). The interference between the direct and reflected signals produces a characteristic pattern in the SNR data that depends on the height of the GPS antenna above the reflecting surface, reflection coefficients for the reflecting surface, and for vegetation sensing, the water content of the vegetation. GPS-IR has a bi-static radar geometry (Figure 1). A GPS satellite transmits primarily Right-Handed Circularly Polarized (RHCP) signals at two frequencies (originally ~1.5 and 1.2 GHz; a third frequency was recently added). For GPS-IR, these will be referred to as the direct signals. A geodetic-quality GPS antenna is designed to preferentially track this direct signal, so the RHCP gains are many orders of magnitude larger than for Left-Handed Circularly Polarized (LHCP) signals. Most of the reflected energy is converted from RHCP to LHCP, with the degree of conversion depending on the surface dielectric constant and the satellite elevation angle. At low elevation angles (< 20 degrees), the RHCP gains begin to taper so that reflections from the ground surface (i.e. negative elevation angles) can be suppressed. The GPS (choke ring) antenna frequently used by the geodetic community has very small LHCP gains at negative elevation angles, and thus does an excellent job of suppressing reflections from surfaces where there is a strong conversion from RHCP to LHCP (e.g. metal surfaces). However, it does a relatively poor job of suppressing reflections from natural surfaces such as soil and snow.

The GPS observation (RINEX) files report SNR data in units of decibels assuming a 1Hz bandwidth, or dB-Hz. The strength of the direct SNR signal depends strongly on:

(1) satellite transmit power
(2) gain pattern of the receiving antenna
(3) whether the code on the transmitted signal is public or encrypted.

The L1 signal includes both a public and encrypted code, whereas the L2 signal was originally designed with only an encrypted code. Because the receiver lacks access to the code, these L2 measurements have much lower power than the equivalent L1 measurements. This makes it more difficult to use older L2 SNR signals for GPS-IR. In contrast, the L1 SNR data extracted from the public codes have strong power levels, but are very noisy, making it also difficult to use these data to measure the reflected signal. This L1 SNR noise is generally attributed to cross-correlation effects between satellites (Lestarquit and Nouvel 2012). Beginning in 2005, GPS began transmitting a new public code on L2 called L2C. It has stronger resistance to satellite cross correlation effects. This paper is based entirely on these new L2C signals. Of the 31 satellites in the current GPS constellation, 11 are transmitting L2C.

SNR observations for a typical L2C satellite observed with a geodetic-quality GPS unit are shown in Figure 2. The observed direct signal (represented by the smooth low-order polynomial fit) rises in strength by 10 dB-Hz as the satellite rises from 5 to 40 degrees elevation angle. This rise in strength is due primarily to a geodetic antenna's gain pattern. The bottom panel of Figure 2 shows the SNR data after the observations have been converted to linear units and the direct signal has been removed with a 2nd order polynomial. The residual SNR trace has a distinctive frequency that depends primarily on the height of the antenna above the reflecting surface (H_o, Figure 1).

$$SNR = A(\theta) * cos\left(\frac{4\pi H_o}{\lambda} sin\theta + \phi_o\right) \cong A * cos(\frac{4\pi H_o}{\lambda} sin\theta + \phi_o) \quad (1)$$

Equation (1) is the fixed reflector height model for GPS-IR. H_o has been referred to as the effective reflector height (Larson et al. 2010; Chew et al. 2013). For bare soil conditions and most soil types, H_o varies 0-5 cm as near-surface soil layers become wet and dry. For soil moisture studies H_o is determined empirically and fixed; A and ϕ_o are then estimated using least squares. Changes in ϕ_o are then related to soil moisture content using electrodynamic models (Chew et al. 2013). For snow and sea level studies, the fixed reflector height model cannot be used. Instead, H_o is estimated using a Lomb Scargle Periodogram to determine the effective reflector height. This is then converted to snow depth or sea level height (Larson and

Nievinski 2013; Larson et al. 2013). None of these previous studies (soil moisture, snow, or sea level) used the amplitude information from *A*.

Technique GPS Issues

Theoretical models show that *A* from the fixed reflector height model will be attenuated by canopies with vegetation water content less than 1 kg/m^2 (Chew et al. in revision); these model results are supported by field observations. For values above 1 kg/m^2, models show that significant reflections from the vegetation itself exist, and the fixed reflector height model for GPS-IR fails. Furthermore, variations in soil moisture are expected to also influence SNR amplitudes (Zavorotny et al. 2010; Chew et al. 2013). However, before we can reliably link estimated values of *A* to vegetation water content (and surface soil moisture), we must also assess GPS-specific error sources that influence *A*.

(1) Equation 1 is an approximation; observed SNR amplitudes still retain a small dependence on elevation angle. This means that inhomogeneities in satellite tracks (i.e. one that begins tracking from an elevation angle of 5 degrees and another starting at 10 degrees) will result in different estimated values of *A*. For an ideal GPS receiver, one would be able to track all satellites in view from the same minimum elevation angle. However, many geodetic GPS systems were designed to track only 8-12 satellites at a time. As the GPS constellation is currently operating 30% beyond its design specifications, many geodetic GPS receivers cannot track all visible satellites. They are programmed to make decisions about the preferred signals to track. Generally the choice is made to drop low elevation angle satellites because these signals produce noisier position estimates. This means inconsistent data sets can inadvertently be collected that show time-varying GPS amplitude signals that have no relation to vegetation water content. Because this study only uses L2C signals, we deliberately turned off tracking of 1-2 healthy GPS satellites so that no L2C data were lost. The choice of which satellite(s) to remove must be made independently for each site because satellite geometry is latitude/longitude dependent.

(2) The GPS system consists of more than 30 satellites, with new satellites being launched on a nearly yearly basis. In the last few years the U.S. Department of Defense has opted to use higher

(~4 dB-Hz) power transmission levels for these newer satellites (Figure 3). If uncorrected, these new power levels will result in larger SNR amplitude values for these satellites, which would bias estimates of vegetation water content. While not a pervasive effect, we have also identified a four day period when the Department of Defense tested out the flexible power transmission capabilities of the new L2C satellites. This meant that power on those days was higher. If these data were not removed, the GPS amplitude data would have been interpreted as having lower vegetation water content.

(3) Multiple components of a GPS instrument show a strong sensitivity to temperature, particularly the antenna pre-amplifier, cables, and the receiver. The latter is generally stored in a plastic box near the antenna, where it is shielded by some, but not all, of the external temperature extremes. Figure 4 shows SNR observations for an extreme case. In the winter example, the air temperature for this satellite track was -15 C, while in summer it was 32 C. There is a clear bias between the winter and summer data of ~1.5 dB-Hz. An analysis of a full year of SNR data shows that SNR data are strongly correlated with air temperature (e.g. Larson 2013). However, the exact relationship between the SNR data and air temperature is difficult to predict because 1) each site different cable lengths, 2) some cables are buried and some are not, and 3) the receivers are shielded from temperature extremes in different ways. Even though the temperature bias appears to be large, once the direct signal component is removed with a polynomial, the discrepancy between summer and winter data is much less apparent. Figure 4 also shows SNR data corrected for temperature using a linear relationship between air temperature and SNR. While the raw SNR data agree much better with each other than the original summer and winter observations, the improvement for the SNR data after the direct signal removed is very small.

Finally, the issue of the GPS reflection footprint needs to be addressed. The GPS-IR footprint for a single rising or setting satellite depends on GPS signal wavelength (for L2C it is ~24 cm), the satellite elevation angle, and H_o. It is an elongated ellipse in the direction of the satellite track (the exact equations are given in Larson and Nievinski (2013)). As the satellite rises and elevation angle increases, the Fresnel zone gets smaller and closer to the GPS antenna. Figure 5 summarizes the general features of the Fresnel zones for GPS satellites available for the time period of 2010-2012. For sites at mid-northern latitudes (~30-40 degrees), there are no satellite

tracks between azimuths of ~315 and 45 degrees. For sites in natural environments, all of the satellite tracks in Figure 5 could be used. For this paper, only the southern tracks will be used because the farmers requested that we deploy the GPS instruments at the northern ends of their agricultural fields. We considered using some of the more easterly and westerly satellite tracks, but opted not to because the fields on either side of our agricultural experiments were either fallow or growing a different crop.

Figure 5 also makes clear that the GPS-IR reflection footprint is far from homogeneous. For an antenna that is 2 meters high and a satellite at elevation angle of 5 degrees, it extends a radial distance of over 60 meters; however, this spatial sampling quickly reduces to ~20 meters at an elevation angle of 10 degrees. Standard retrievals using GPS-IR have used elevation angle ranges of 5-30 degrees to ensure that the frequency of the SNR data can be reliably retrieved (Larson et al. 2010; Larson and Nievinski 2013). This means that a large percentage of the data are collected within 10 meters of the antenna. The sampling footprint can easily be increased in size by raising the height of the GPS antenna, but this does not make the footprint homogeneous.

Previous GPS-IR analyses have assumed that the Fresnel zones for a reflection experiment do not vary. Figure 6 shows that this is a good assumption. Except for one satellite, the GPS-IR footprint varies by only 3-5 meters. In 2010 satellite 15 shows a spread of ~10 meters in its footprint. This is indicative of orbit maneuvering by the U.S. Department of Defense. This was the only significant change between 2010 and 2012 for the 7 satellites used in this study.

The analysis of the GPS SNR data can be summarized as follows:

1. For each day, the direct signal of the SNR data for the satellite tracks (as shown in Figure 2) was removed with a 2nd order polynomial. The residual, using a linear scale, was fit to equation (1), i.e. the fixed reflector height model. Least squares was used to estimate A and ϕ_o. The effective reflector height that defines H_o for each satellite track was estimated using ~30 days of bare soil conditions and fixed throughout.

2. To remove effects of variable transmit power, the estimated amplitudes for each satellite track were normalized relative to their bare soil values ($A_{norm} = A/A_{baresoil}$). Thus, normalized amplitude values of 1 are for bare soil.
3. A daily amplitude value was then constructed using the mean of the individual normalized satellite amplitudes.
4. For agricultural sites, the data before and after the fields were plowed (which changes surface roughness and the effective reflector height), were discarded. For all sites data impacted by snow were removed.

GPS Data

We used data from five sites in this study. Two GPS receivers were deployed at the Sevilleta Long-Term Ecological Research Station in New Mexico (http://sev.lternet.edu). One measured a desert grassland and the other receiver was installed in a shrubland. The remaining field sites were located near Boulder, Colorado. The first, Marshall Field, has vegetation characterized as short-grass steppe. The other GPS receivers were deployed in agricultural fields. One of these sites was planted with alfalfa in each of the years from 2010-2012. The crop was harvested 3-4 times each summer. The other site was located near a wheat field in 2010 and 2011 and an oat crop in 2012. For simplicity, we will always call this the wheat site. Only one crop is harvested each year at the wheat site; it is not irrigated. All of the sites had identical GPS equipment: a Trimble netRS geodetic-quality dual-frequency receiver. The choke-ring antenna was covered by a radome. The receivers all operated at 1 sample per second and tracked the new L2C signal as well as the legacy L1 and L2 signals. They were 2 to 2.4 meters above the ground. As will be discussed later, there were drought conditions in Boulder in 2012. This significantly affected all the data collected in Boulder that year.

In Situ Data

During the growing season at the Boulder sites, *in situ* data were measured on a nearly weekly basis (Figure 7). A 30 cm by 30 cm quadrat was thrown randomly in 7 different locations within 7-35 meters from the GPS antenna. The distances and azimuths were recorded. For each vegetation sample, the plants within the quadrant were clipped and weighed immediately. This will be called the wet weight. The samples were bagged, dried in an oven for 48 hours at 50^{o}C,

and then weighed again; this is the dry weight. Vegetation water content is the difference between the wet weight and dry weight. It should be noted that the sampling procedure changed between 2010 and following years. In 2010, we sampled between 7-75 meters from the GPS antenna; whereas in subsequent years, we only sampled between 7-35 meters (as stated above). This was due to the fact that, at the end of 2010, we refined our Fresnel zone estimates and concluded that most of the reflected signal was actually coming from closer to the antenna. We also collected *in situ* vegetation data more frequently in 2011 and 2012 than we did in the first field season.

Although we compute statistics for these *in situ* vegetation measurements, we cannot expect the means or standard deviations to completely characterize the state of vegetation on any given day. The natural environment surrounding most GPS antennas includes widely varying vegetation cover, even within one field site. The inhomogeneous vegetation that exists is not guaranteed to follow a normal distribution, and seven samples are not enough to determine whether any such distribution exists. However, taking more samples could have significantly altered the field sites over time and thus altered our conclusions in this study. Despite this, we do see seasonal variations in our vegetation measurements and therefore use them to interpret our results in a general sense.

Vegetation height was also measured at each site. For these measurements, we recorded the 90% canopy height. This was done so as to minimize anomalously high measurements that could have been caused by reporting the absolute maximum height. Figure 7 summarizes the *in situ* vegetation measurements. At Marshall the vegetation water contents peaked at ~0.5 kg/m^2 in 2010 and 2011, but show almost no growth during the drought year in 2012. Average height values are below 40 cm. At the wheat site in 2010-2011, water content values range from 0-0.9 kg/m^2 and peak heights were also slightly higher than at Marshall, ~80 cm. However, the wheat crop in 2012 was drastically impacted by the drought, with significantly lower heights and water content. At the alfalfa field, vegetation water content measurements are almost ten times higher, reaching as values of 4.5 kg/m^2. This is because the farmers irrigate the alfalfa field, but not the wheat field. Vegetation heights peaked at ~100 cm.

Results

Following the protocol described in the previous section, time series of normalized GPS amplitude time series for each GPS satellite were estimated for each field site for the years 2010, 2011, and 2012. Before assessing the relationship between mean GPS amplitudes and vegetation growth, we will first use these time series to assess the internal consistency of the solutions. The average normalized GPS amplitudes will produce an unbiased estimate of amplitude if the individual satellite track retrievals are themselves unbiased. This assumption can be tested by assessing the agreement between individual satellite amplitude retrievals. Figure 8 compares the normalized amplitude retrievals over three years for satellites 5 and 29 at Marshall Field; these satellites have adjacent footprints. There is a small bias of 0.05 for all three years (normalized amplitude units). Although the temperature dependence appeared to be small, we also compared three years of solutions for Marshall Field. The impact of an uncorrected temperature bias is even smaller, 0.01 in normalized amplitude units (Figure 8).

Representative GPS amplitude time series for the four field sites (Sevilleta shrublands, Marshall, wheat, and alfalfa) are shown in Figure 9. Sevilleta amplitudes vary little from a bare soil value of 1. This is consistent with a limited number of *in situ* measurements made in 2010, where vegetation water content was ~0.01-0.02 kg/m^2. The largest amplitude excursions in the GPS amplitude time series coincide with precipitation, as shown in the middle panel. The quick "dry downs" correlate strongly with *in situ* measurements of soil moisture (not shown). Note that the GPS amplitudes are smaller after it rains at the Sevilleta site. The lower panel shows the dominant effective reflector height (estimated using the Lomb Scargle Periodogram) relative to the A we used in the fixed reflector height model (estimated using Least Squares). At the Sevilleta site, effective reflector height varies by less than a cm – and only at times when the precipitation gauge indicates that it rained. This is consistent with electrodynamic forward models (Zavorotny et al. 2010, Chew et al. 2013) and field observations (Larson et al. 2010).

At Marshall the normalized GPS amplitudes (Figure 9) roughly agree with the growing cycle seen in the *in situ* data (Figure 7). In contrast with Sevilleta, changes in effective reflector height are much more pronounced at this site. These appear highly correlated with precipitation events, and the expected attendant changes in soil moisture. At the wheat site, the GPS amplitudes are

307 also consistent in timing with the *in situ* vegetation data. However, those GPS amplitude changes
308 are mirrored by changes in reflector height variations. As the wheat crop grows, the estimated
309 reflector height gets closer to the antenna by 3-4 cm. It returns closer to its initial value after the
310 crop is harvested. There is also a large positive excursion at approximately day of year 175. This
311 correlates with a large precipitation event. Again, this is consistent for soil moisture variations
312 with a vegetation canopy (Chew et al. in revision). Note that the excursion associated with soil
313 moisture signal for a vegetated soil surface (Marshall, Wheat) has the opposite sign from that of
314 bare soil (Sevilleta).
315
316 Finally, we examine the GPS amplitude retrievals for alfalfa. Except for a few weeks between
317 each of the alfalfa crops, the dominant reflector height (shown in the bottom panel) is far from
318 the effective reflector height used to estimate those amplitudes. In other words, the constant
319 reflector height model used to derive these amplitudes is invalid because the reflector height used
320 in least-squares estimation of amplitude is not close to the dominant reflector height in the SNR
321 data. We can see more detail of how the constant reflector height model breaks down in Figure
322 10. Here the estimated reflector height values are plotted as a function of the *in situ* vegetation
323 water content (interpolated from the field data). When the vegetation water content value is low
324 (0-0.5 kg/m^2), GPS amplitude values are relatively close to bare soil values (0.8-1.0). However,
325 as vegetation water content increases, the GPS amplitudes quickly drop, and the dominant
326 effective reflector height observed in the SNR data moves closer to the antenna, i.e. in the
327 direction of vegetation growth. Again, this result is consistent with forward models (Chew et al.
328 in revision).
329
330 Figures 11 and 12 summarize the amplitude-vegetation water content relationship for the
331 Marshall and wheat fields. The uncertainties shown are based only on repeatability (i.e. the
332 standard deviation of the observations, rather than the standard deviation of the mean). While the
333 measurements in 2011 are fairly consistent, the 2010 measurements show very poor agreement
334 between the GPS results and *in situ* data. While the measurement protocol changed between
335 2010 and 2011 to emphasize the region closer to the GPS antenna, it is not clear that this is
336 responsible for the discrepancy. The *in situ* measurements in 2010 were also less precise than in
337 subsequent years. There is almost no measured vegetation water content in 2012. Using all three

years of data, the R^2 value is 0.3. The wheat data show a much stronger correlation between the GPS and *in situ* data, with a R^2 0.7. Some of the misfit between GPS and the *in situ* data is caused by soil moisture variations. This error is predicted to be on the order of 0.1-0.2 kg/m^2. For these field studies that would translate to an error of 10-20% for vegetation water content estimates (Chew et al. in revision).

The amplitudes of GPS SNR data are clearly sensitive to vegetation growth in general, and vegetation water content specifically. However, SNR data are also sensitive to soil moisture content, which complicates our ability to isolate vegetation water content. Furthermore, the gain pattern of a geodetic antenna is a significant restriction on using this system for vegetation monitoring. Other GPS-IR applications (snow and sea level) were primarily geometry driven, meaning that the frequency of the SNR interference pattern was used. SNR phase retrievals have also been shown to be robust for soil moisture (Larson et al. 2010; Chew et al 2013). However, SNR amplitudes are sensitive to multiple factors. This makes it difficult to uniquely derive vegetation water content using GPS-IR. While a geodetic GPS receiver could still be used, an antenna that was designed to measure vegetation growth - analogous to the ones used by in GPS vegetation monitoring experiments (Rodriguez-Alvarez et al. 2011; Egido et al. 2012) - would yield stronger results. One side benefit of the GPS SNR amplitudes shown here (and the associated effective reflector heights) is that they can be used to identify times when soil moisture estimates derived using GPS-IR have been contaminated by vegetation growth.

Conclusions

This study assesses the agreement between GPS reflection data and measured vegetation water content for three years of data from natural environments and agricultural fields. The GPS instrument used in the experiments is not designed for vegetation sensing; it is most typically used by geodesists and surveyors. A normalization method is proposed to minimize the effect of satellite track inhomogeneities. The influence of temperature on the GPS data was evaluated and found to be small compared to the typical noise in the GPS SNR data. The GPS data are sensitive to the water content in plant types such as desert grasses and agricultural crops such as wheat. However, the very simple model used to model variations in amplitude breaks down in

water-laden crops such as alfalfa. This is consistent with model predictions (Chew et al. in revision), restricting its use for vegetation water contents of less than ~1 kg/m^2.

Acknowledgements

The first author's visit to the University of Colorado was funded by China Scholarship Council, File No. 201206010122. The University of Colorado was funded by NSF AGS0935725 and EAR1144221.

References

Chew CC, Small EE, Larson KM, Zavorotny VU (2013) Effects of Near-Surface Soil Moisture on GPS SNR Data: Development of a Retrieval Algorithm for Soil Moisture. IEEE Trans Geosci Rem Sens PP (99):1-7. doi:10.1109/TGRS.2013.2242332

Chew CC, Small EE, Larson KM, Zavorotny VU Utility and limitations of GPS-Interferometric Reflectometry in vegetation sensing. IEEE Trans Geosci Rem Sens. In revision.

Egido A, Caparrini M, Ruffini G, Paloscia S, Santi E, Guerriero L, Pierdicca N, Floury N (2012) Global Navigation Satellite Systems Reflectometry as a Remote Sensing Tool for Agriculture. Rem Sens 4 (8):2356-2372. doi:10.3390/rs4082356

Garrison JL, Komjathy A, Zavorotny VU, Katzberg SJ (2002), Wind speed measurement using forward scattered GPS signals, *IEEE Trans. Geosci. Remote Sens.*, 40(1): 50–65.

Garrison JL, Katzberg SJ (2000) The Application of Reflected GPS Signals to Ocean Remote Sensing. Rem Sens Environ 73 (2):175-187. doi:10.1016/s0034-4257(00)00092-4

Gleason S, Hodgart S, Yiping S, Gommenginger C, Mackin S, Adjrad M, Unwin M (2005) Detection and Processing of bistatically reflected GPS signals from low Earth orbit for the purpose of ocean remote sensing. IEEE Trans Geosci Rem Sens 43 (6):1229-1241. doi:10.1109/TGRS.2005.845643

Joseph A (2010) Measuring GNSS Signal Strength-What is the difference between SNR and C/N0?. Inside GNSS:20-25

397 Katzberg SJ, Torres O, Grant MS, Masters D (2005) Utilizing calibrated GPS reflected signals to
398 estimate soil reflectivity and dielectric constant: Results from SMEX02. Rem Sens Environ
399 100 (1):17-28. doi:10.1016/j.rse.2005.09.015
400 Larson KM (2013) A Methodology to Eliminate Snow and Ice-Contaminated Solutions from
401 GPS Coordinate Time Series, J. Geophys. Res, Vol. 118(8):4503-4510.
402 doi:10.1002/jgrb.50307
403 Larson KM, Small EE, Gutmann ED, Bilich AL, Braun JJ, Zavorotny V (2008) Use of GPS
404 receivers as a soil moisture network for water cycle studies. Geophys Res Lett 35:L24405.
405 doi:10.1029/2008GL036013
406 Larson KM, Gutmann ED, Zavorotny V, Braun A, Williams MW, Nievinski FG (2009) Can we
407 measure snow depth with GPS receivers. Geophys Res Lett 36:L17502.
408 doi:10.1029/2009GL039430
409 Larson KM, Braun JJ, Small EE, Zavorotny VU, Gutmann ED, Bilich AL (2010) GPS Multipath
410 and Its Relation to Near-Surface Soil Moisture Content. IEEE JSTARS 3 (1):91-99.
411 doi:10.1109/JSTARS.2009.2033612
412 Larson KM, Löfgren JS, Haas R (2013) Coastal sea level measurements using a single geodetic
413 GPS receiver. Adv Space Res 51 (8):1301-1310.
414 doi:http://dx.doi.org/10.1016/j.asr.2012.04.017
415 Larson KM, Nievinski FG (2013) GPS snow sensing: results from the EarthScope Plate
416 Boundary Observatory. GPS Solut 17 (1):41-52. doi:10.1007/s10291-012-0259-7
417 Lestarquit L, Nouvel O (2012) Determining and measuring the true impact of C/A code cross-
418 correlation on tracking—Application to SBAS georanging;Application to SBAS
419 georanging. In: Position Location and Navigation Symposium (PLANS), Proc IEEE/ION
420 PLANS. pp 1134-1140. doi:10.1109/PLANS.2012.6236968
421 Martin-Neira M (1993) A Passive Reflectometry and Interferometry
422 System(PARIS)-Application to ocean altimetry. ESA Journal 17 (4):331-355
423 Notarnicola C, Posa F (2007) Inferring Vegetation Water Content From C- and L-Band SAR
424 Images. IEEE Trans Geosci Rem Sens 45 (10):3165-3171. doi:10.1109/TGRS.2007.903698
425 Rodriguez-Alvarez N, Camps A, Vall-llossera M, Bosch-Lluis X, Monerris A, Ramos-Perez I,
426 Valencia E, Marchan-Hernandez JF, Martinez-Fernandez J, Baroncini-Turricchia G, Perez
427 G, C., Sanchez N (2011) Land Geophysical Parameters Retrieval Using the Interference

428 Pattern GNSS-R Technique. IEEE Trans Geosci Rem Sens 49 (1):71-84.
429 doi:10.1109/TGRS.2010.2049023
430 Rodriguez-Alvarez N, Bosch-Lluis X, Camps A, Ramos-Perez I, Valencia E, Hyuk P,
431 Vall-llossera M (2012) Vegetation Water Content Estimation Using GNSS Measurements.
432 IEEE Geosci Rem Sens Lett 9 (2):282-286. doi:10.1109/LGRS.2011.2166242
433 Segall P, Davis j (1997) GPS applications for geodynamics and earthquake studies. Ann Rev
434 Earth Planet Sci 25:301-336. doi:10.1146/annurev.earth.25.1.301
435 Small EE, Larson KM, Braun JJ (2010) Sensing vegetation growth with reflected GPS signals.
436 Geophys Res Lett 37 (12):L12401. doi:10.1029/2010GL042951
437 Zavorotny VU, Larson KM, Braun JJ, Small EE, Gutmann ED, Bilich AL (2010) A Physical
438 Model for GPS Multipath Caused by Land Reflections: Toward Bare Soil Moisture
439 Retrievals. IEEE JSTARS 3 (1):100-110. doi:10.1109/JSTARS.2009.2033608
440

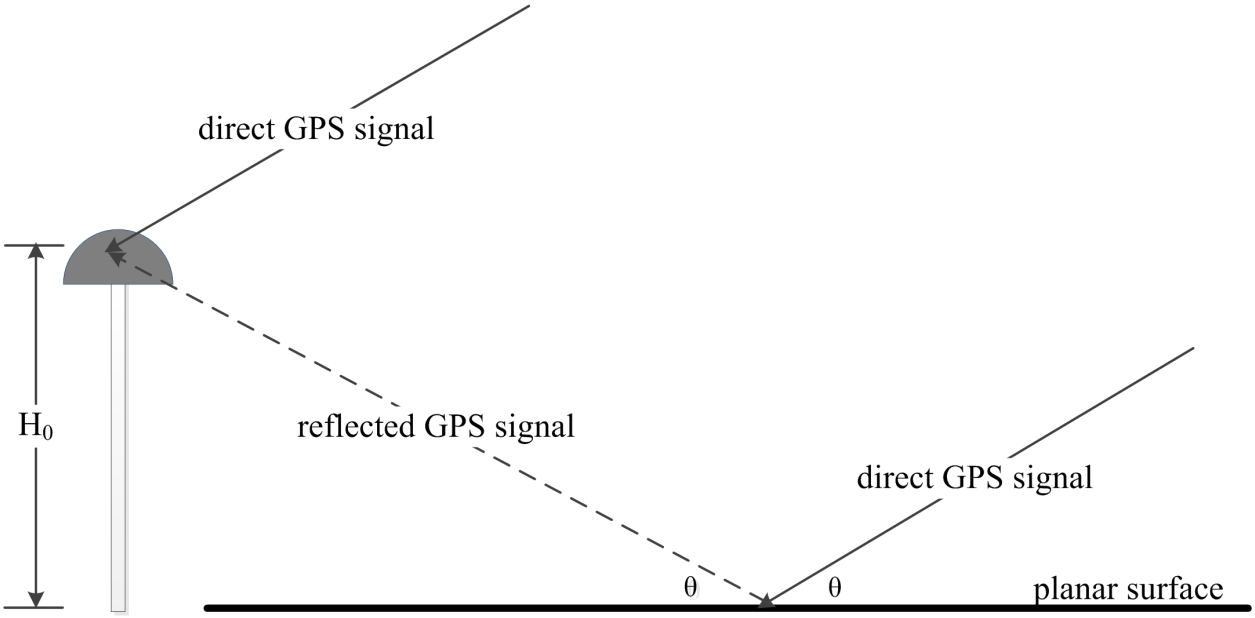

Figure 1. Bi-static geometry of GPS-IR. θ is elevation angle of the satellite with respect to the horizon, H_o is the apparent height of the GPS antenna phase center (depicted by the gray hemispherical dome) above the reflecting surface.

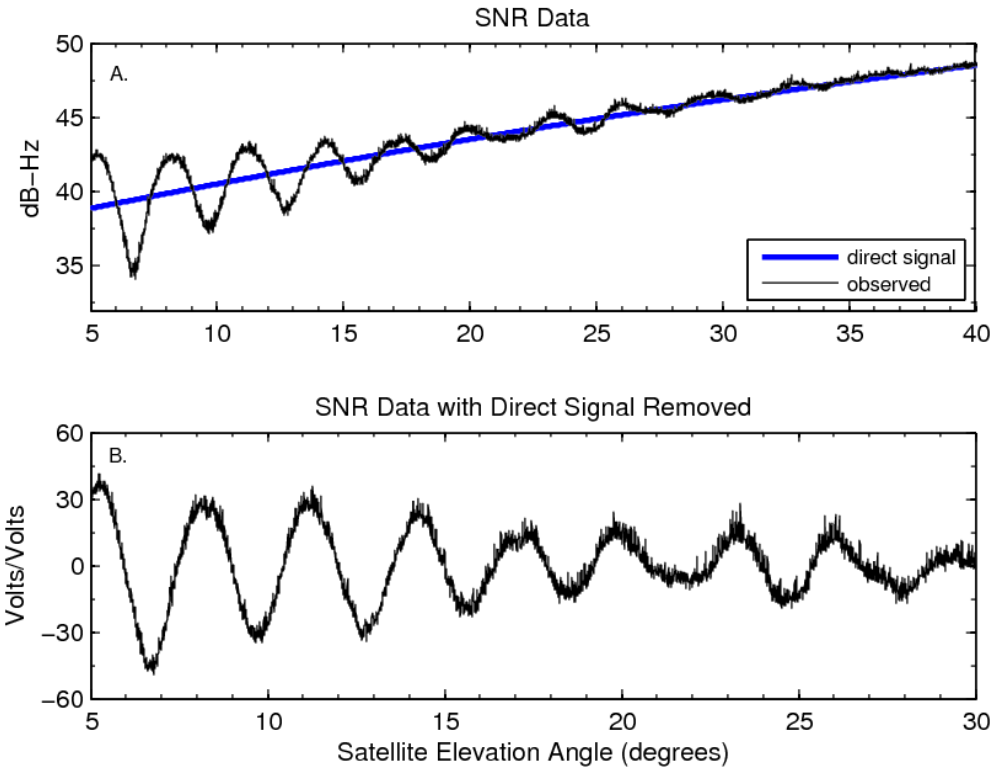

449

450 Figure 2A. L2C SNR data for one GPS satellite are shown in black. The direct signal is
451 represented by the smooth curve in blue; B. SNR data with the direct signal removed and
452 converted to a linear scale. Representative SNR data for older GPS signals (the public L1 C/A-
453 code and encrypted L2 P-code) can be found in Larson et al. (2010).

454

455

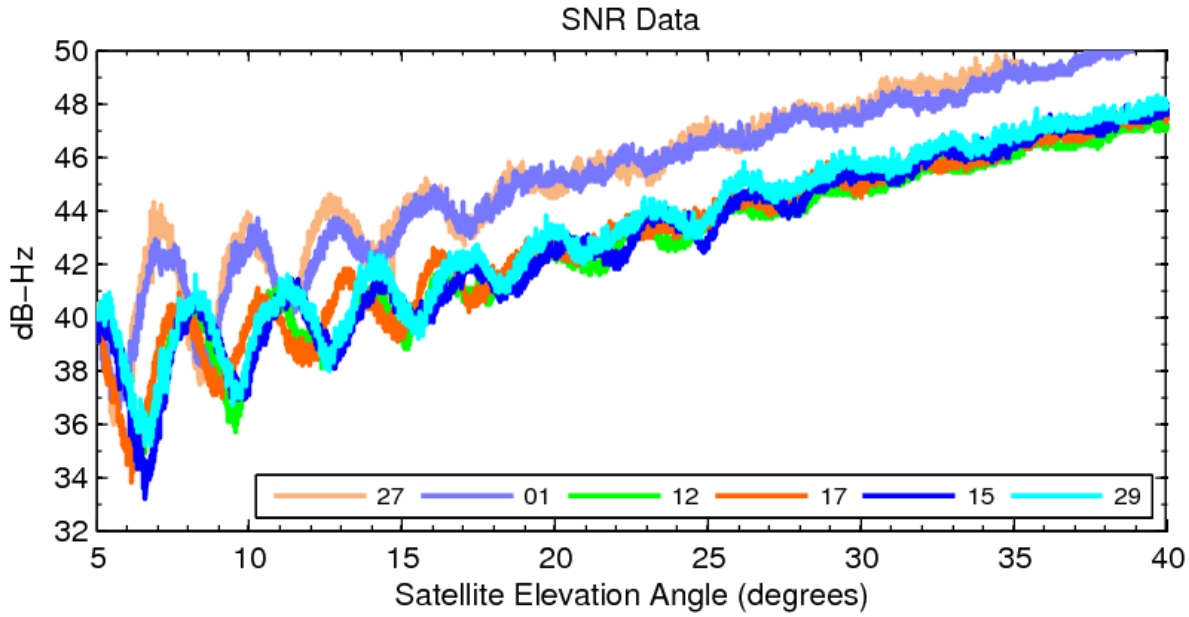

456

457

458 Figure 3. Observed L2C SNR data for six GPS satellites.

459

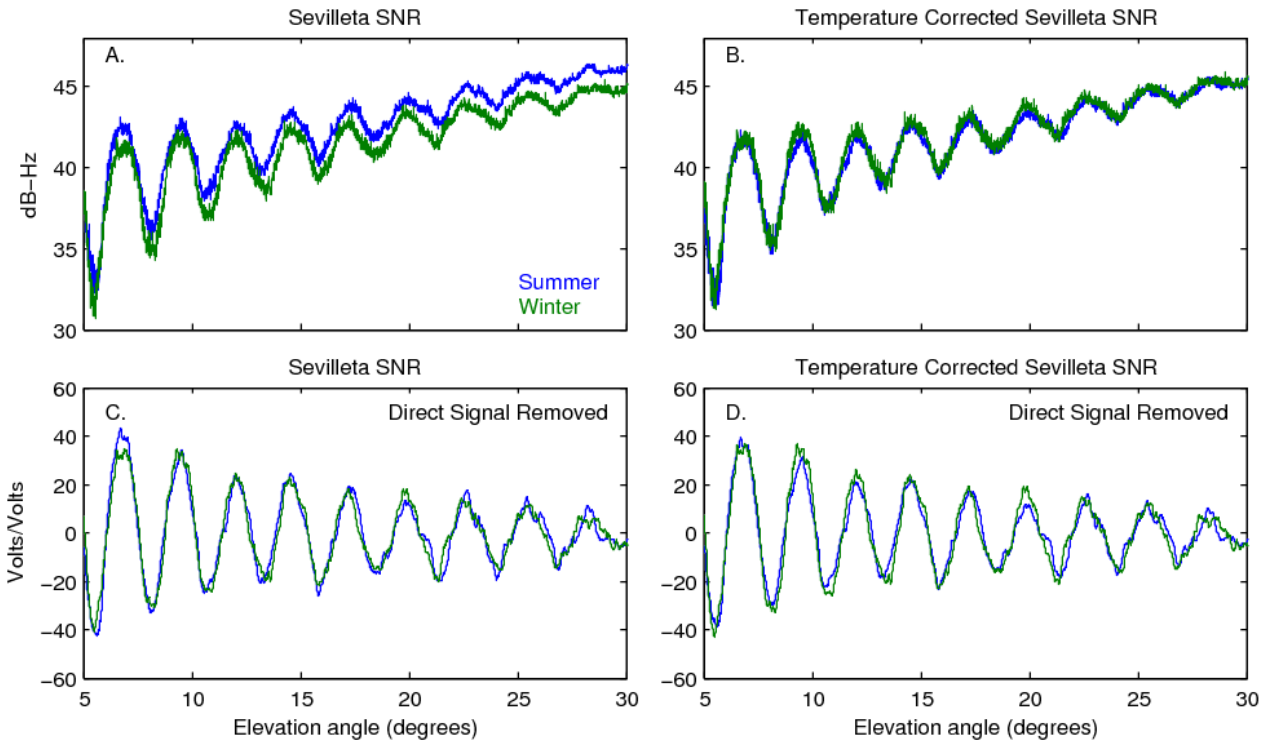

Figure 4A. L2C SNR data in dB-Hz for the Sevilleta grasslands site for representative winter and summer days; B. L2C SNR data corrected assuming a linear relationship between SNR data and temperature; C. SNR data converted to a linear scale with direct signal removed; D. Temperature corrected SNR data converted to a linear scale with direct signal removed. A 15-point smoother has been run on the linear scale data.

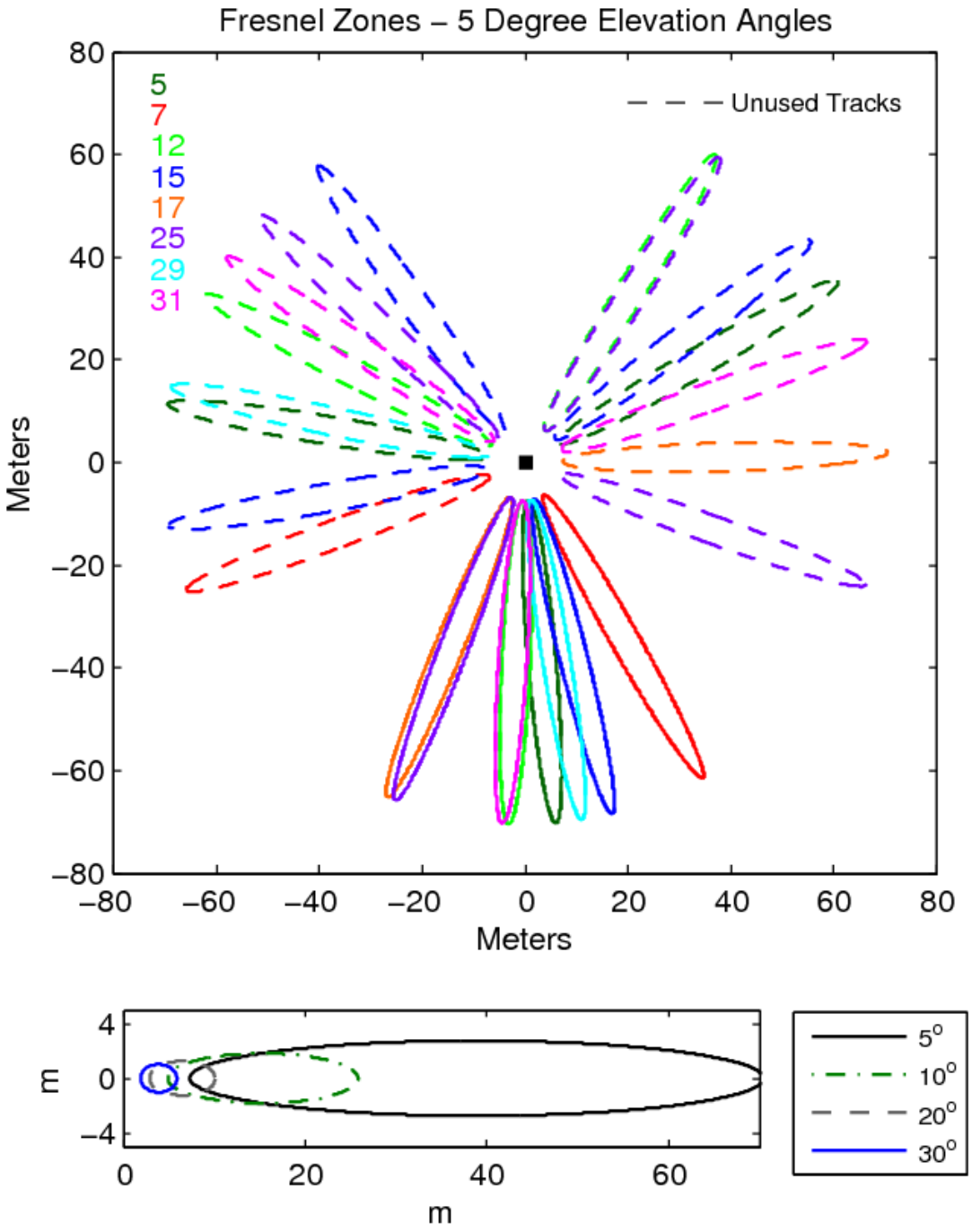

Figure 5. Top: First Fresnel zones computed for an elevation angle of 5 degrees for a GPS antenna that is 2 meters tall and situated at Marshall, Colorado. The satellite numbers used in this study are shown on the left. The GPS antenna is located at the coordinates 0,0. Dashed lines

474 indicate Fresnel zones for satellites tracks that are not used; Bottom: Fresnel zones for elevation
475 angles of 5, 10, 20 and 30 degrees. The GPS antenna is again located at the coordinates 0,0.
476

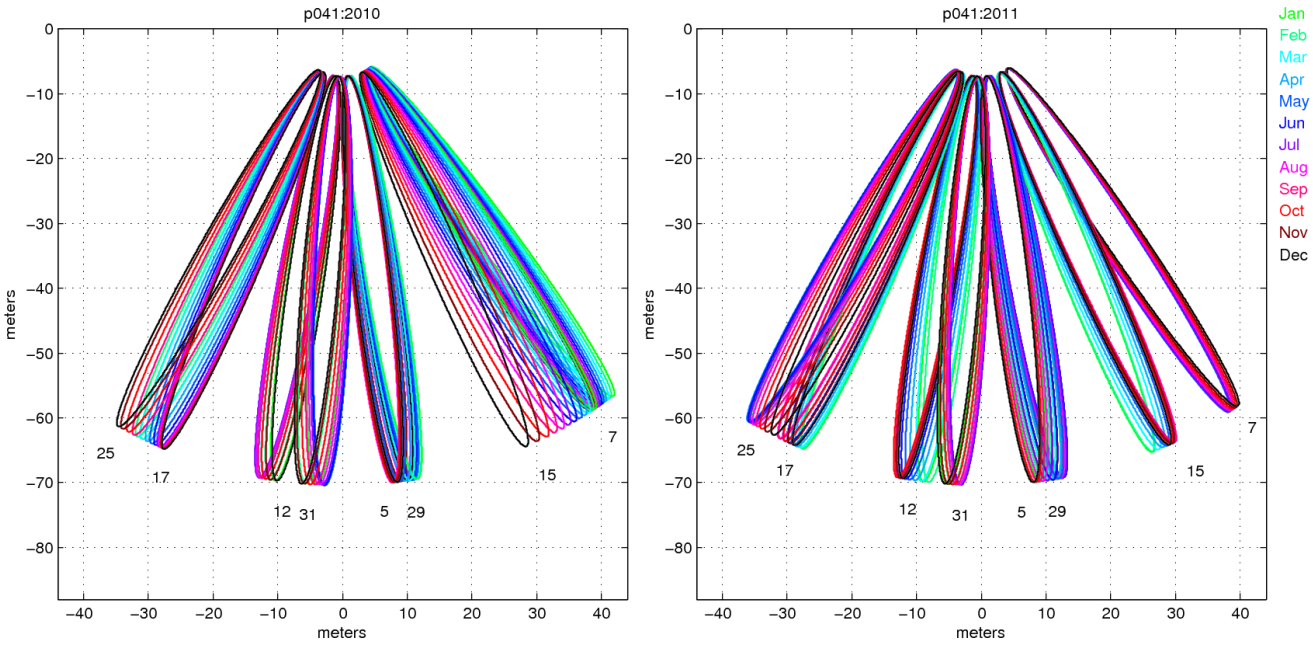

477

478 Figure 6. First Fresnel zones computed each month for 2010 and 2011 at Marshall Field,
479 Colorado. The assumed antenna height is 2 meters and the elevation angle depicted is 5 degrees.
480

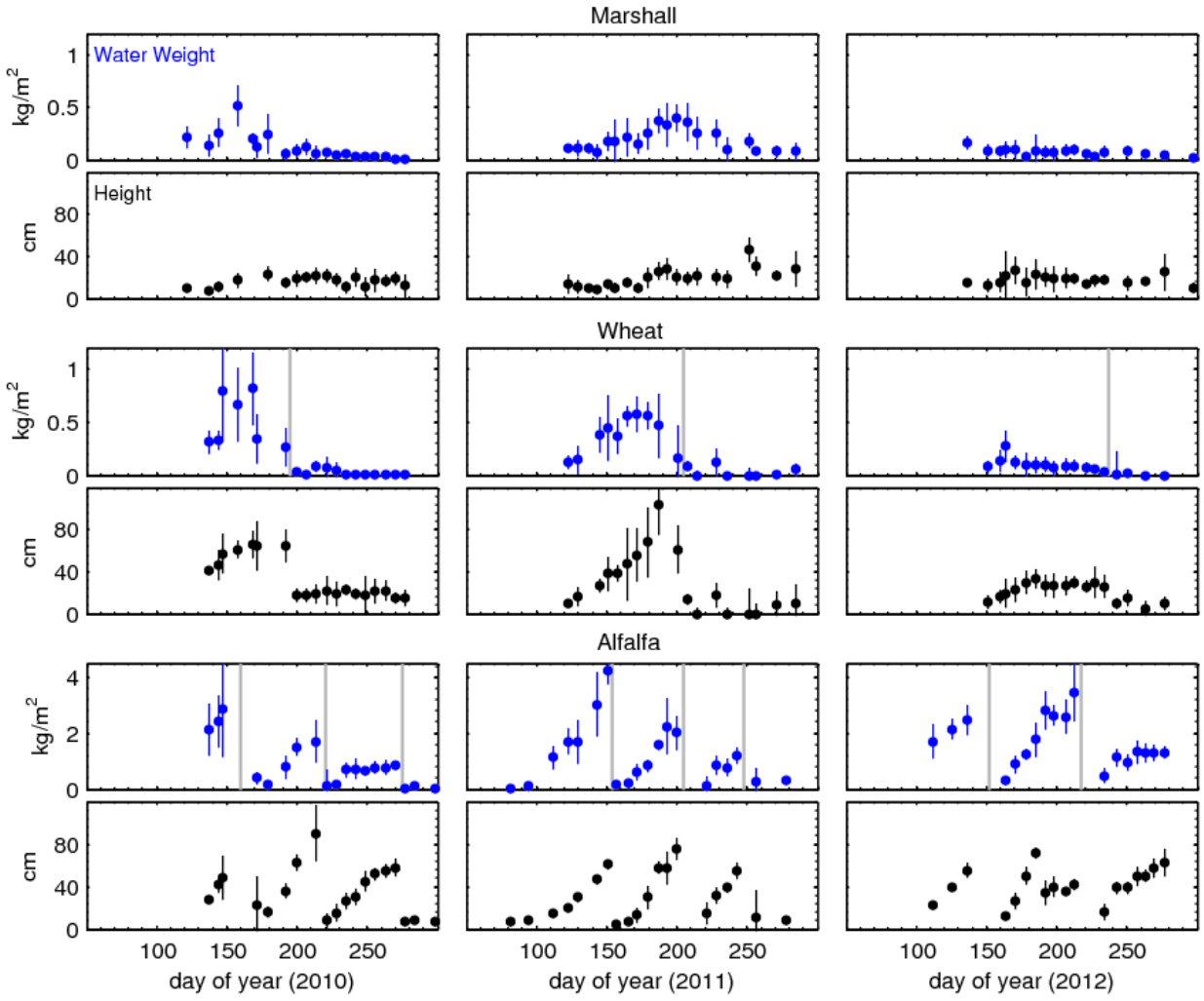

Figure 7. *In situ* field measurements of vegetation water content and vegetation height. Each measurement is the mean and the error bar represents the standard deviation of the individual measurements. Gray lines indicate the approximate timing of the crop harvest.

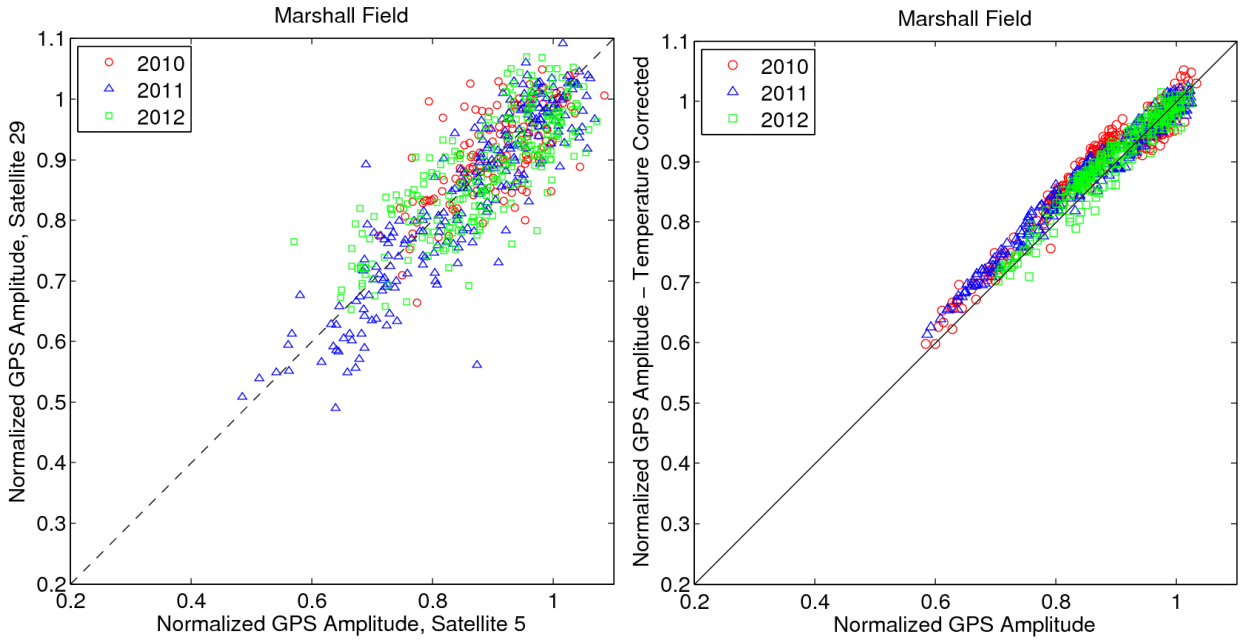

488

489

490 Figure 8. Left: Comparison of normalized amplitude retrievals for satellites 5 and 29 at Marshall
491 Field between 2010 and 2012; Right: comparison of normalized amplitudes, with and without a
492 temperature correction.

493

494

495

496

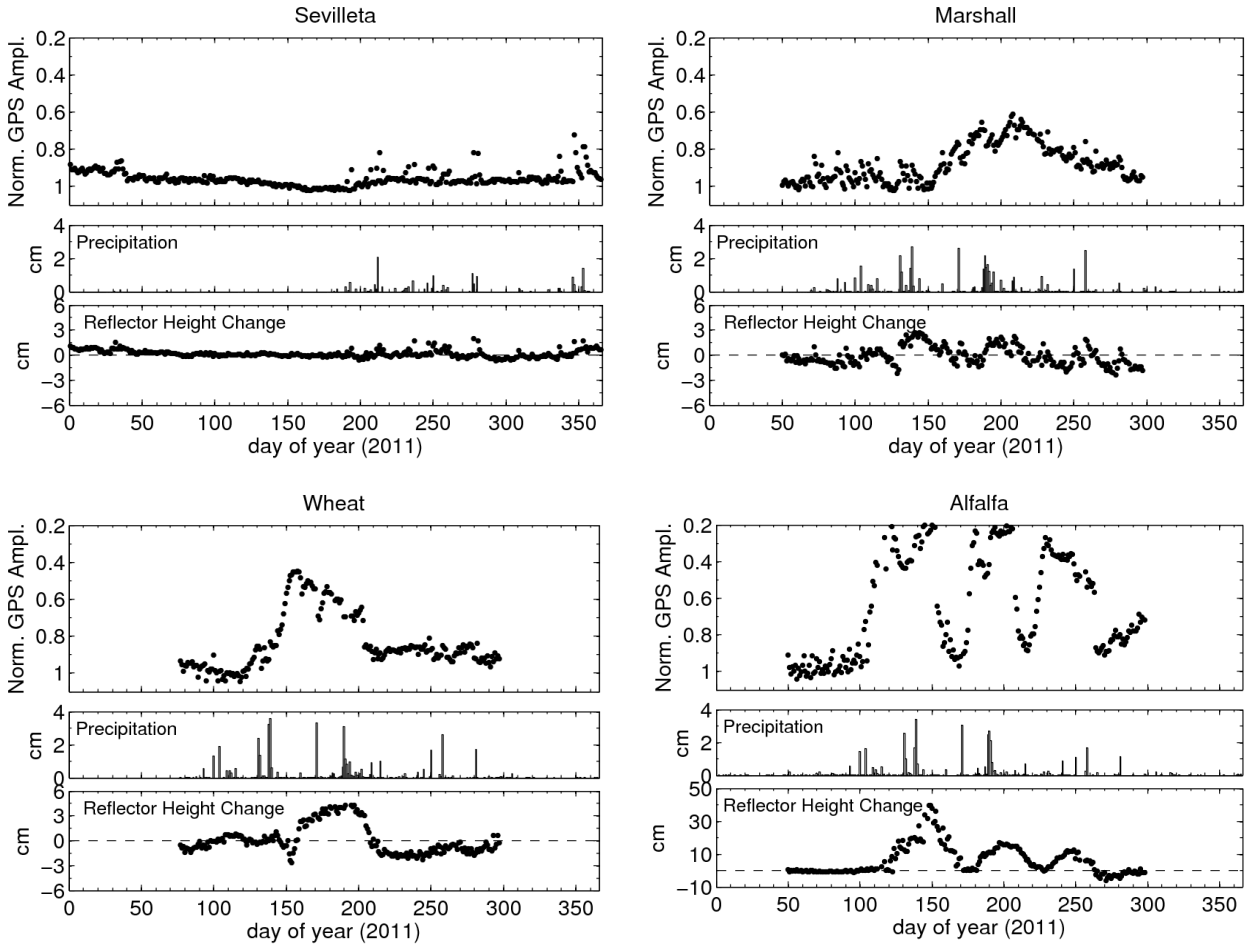

Figure 9. Top panels: normalized GPS amplitudes for Sevilleta shrubland, Marshall, wheat, and alfalfa sites in 2011; middle panel: daily precipitation values; bottom: estimated effective reflector height. Note change in the reflector height change scale for the Alfalfa field.

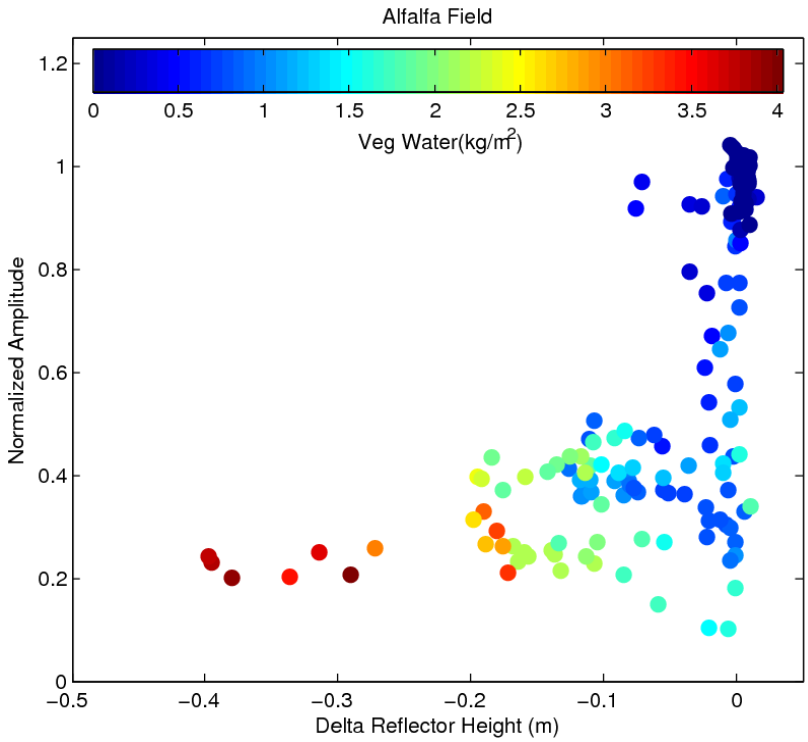

Figure 10. Change of effective reflector height estimated for the alfalfa field in 2011 are compared with normalized GPS amplitude. Color coding at top shows interpolated values for measured vegetation water content.

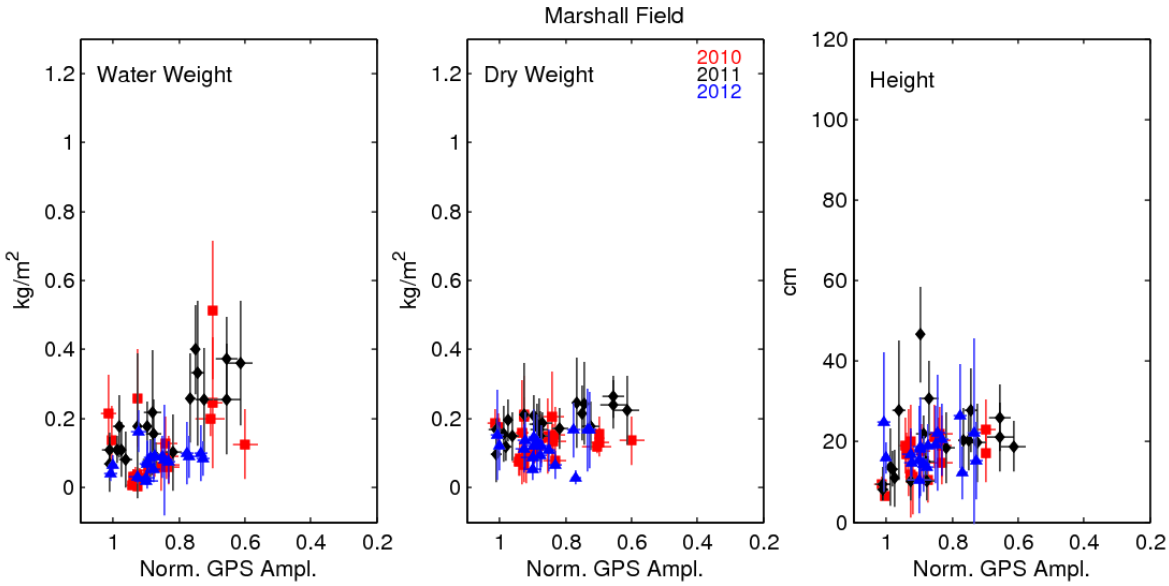

Figure 11. GPS amplitude-vegetation relationships for the Marshall field. From left to right: water weight, dry weight, and height. Both the GPS uncertainties and the *in situ* vegetation water weight uncertainties are based on the observation standard deviation (repeatability). The rergression yields $VWC = -0.51A_{norm} + 0.56$.

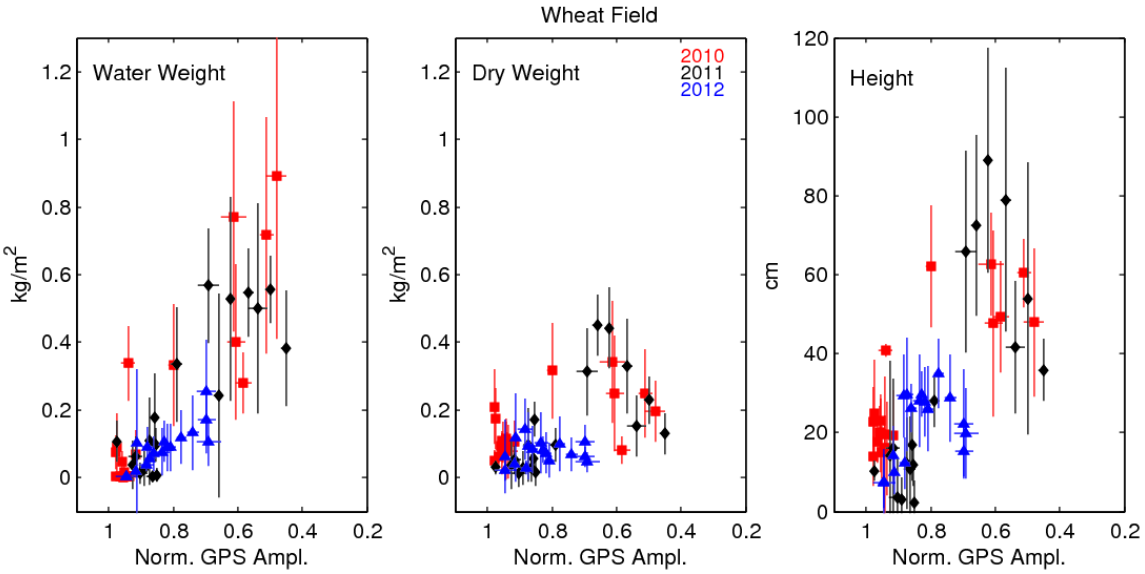

Figure 12. GPS amplitude-vegetation relationships for the wheat field. From left to right: water weight, dry weight, and height. Both the GPS uncertainties and the *in situ* vegetation water weight uncertainties are based on the observation standard deviation (repeatability). The regression yields $VWC = -1.18A_{norm} + 1.13$.